

Imaging Bacteriophage T4 on Patterned Organosilane Monolayers by Scanning Force Microscopy[†]

Jiyu Fang and Charles M. Knobler*

Department of Chemistry and Biochemistry, University of California, Los Angeles, California 90095-1569

Mari Gingery and Frederick A. Eiserling

Department of Microbiology and Molecular Genetics, University of California, Los Angeles, California 90095-1489

Received: March 25, 1997; In Final Form: May 30, 1997[®]

A patterned organosilane monolayer consisting of CH₃-terminated islands surrounded by a CF₃-terminated continuous phase is used as a template for controlling the adsorption of biological molecules. In coadsorption of bovine serum albumin (BSA) and bacteriophage T4 and its tail, the T4 adheres to the CF₃-terminated surfaces while the BSA is restricted to the CH₃-terminated islands. The strong affinity of the T4 for the continuous phase allows detailed imaging by scanning force microscopy in both topographic and frictional force modes. Structural features of the tail tubes are clearly recognized. The baseplates at end of the tubes exhibit different configurations, and in images of T4 obtained by frictional force one can clearly distinguish head, neck, tail, baseplate and fibers. For giant T4 with elongated heads, the surface lattice of the head and the sheath annuli of the tail are resolved in some detail.

Introduction

Atomic force microscopy (AFM) is a promising tool for the study of biopolymers.¹ It allows images of biological materials adsorbed on solid supports to be obtained merely by scanning a probe tip over the sample surface. During the past several years, significant advances in AFM imaging of biological materials in vacuum, air, or liquid environments have been achieved. The method cannot be applied however, if the AFM tip displaces or dislodges the molecules being imaged. Strategies for anchoring biopolymers to surfaces have included covalent bonding of proteins to an adsorbed lipid membrane² and the attachment of DNA to a mica surface that has been treated with magnesium acetate.³ Self-assembled monolayers (SAMs) and Langmuir–Blodgett (LB) films can be employed to produce surfaces with specific adsorption characteristics and lateral organization.^{4,5} High-resolution AFM images have been obtained for biomolecules immobilized on such monolayers.^{6–9}

Recently, we described a method for the preparation of organosilane SAMs with a well-defined lateral distribution of CH₃- and CF₃-terminal groups¹⁰ and showed that bovine serum albumin (BSA) is preferentially adsorbed on the CH₃-terminated parts of the surface. The bacteriophage T4 consists of an elongated icosahedral head, a rod-shaped tail, and a hexagonal baseplate with six fibers.¹¹ Because it has identifiable structures and well-established dimensions, it has been used as a reference sample to test the image capabilities of AFM.^{12–14} In this paper we show that T4 and its tail are preferentially adsorbed on the CF₃-terminated surface of these monolayers, which allows mixtures of BSA and T4 to be spatially separated. Moreover, we find that the adsorption of T4 on the CF₃-terminated surface is sufficiently strong to allow imaging of the bacteriophage by scanning force microscopy and that the resolution in the frictional force mode is significantly higher than that previously achieved in topographical images of T4.

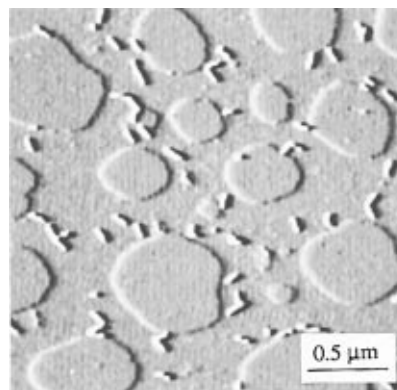


Figure 1. AFM images of tail tubes adsorbed on a patterned OTS/FTS monolayer. OTS islands were prepared by LB deposition at a surface pressure of 5 mNm⁻¹ and a transfer speed of 10 mm min⁻¹. The continuous FTS monolayer was formed by self-assembly. The tubes are adsorbed only on the CF₃-terminated surface.

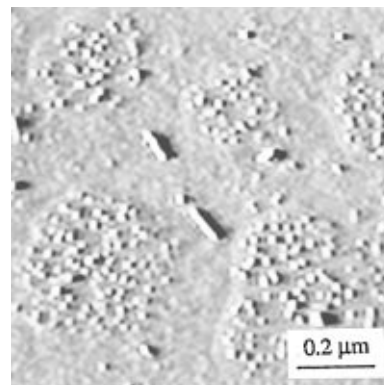


Figure 2. AFM image of coadsorbed T4 tubes and BSA. The BSA is found exclusively on the CH₃-terminated islands and the T4 on the CF₃-terminated continuous phase.

Experimental Section

Octadecyltrichlorosilane (OTS) (Aldrich, 95%) and 1*H*,1*H*,2*H*,2*H*-perfluorodecyltrichlorosilane (FTS) (PCR, 97%)

[†]Dedicated to Professor Daniel Kivelson on the occasion of his 67th birthday.

[®] Abstract published in *Advance ACS Abstracts*, October 1, 1997.

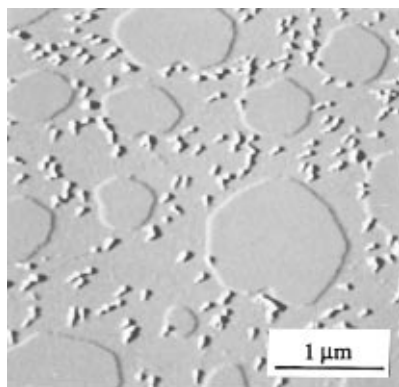


Figure 3. AFM image of tube-baseplates deposited from a $0.1 \mu\text{g/mL}$ solution onto the patterned monolayer. The preparation of the monolayer is described in Figure 1. T-shaped tube-baseplates are found only on the CF_3 -terminated surface.

were used as received. The solvents chloroform and toluene (Fisher, $\geq 99\%$) were dried with molecular sieves prior to use. Water utilized in the experiments was purified by a Millipore Milli-Q system ($18 \text{ M}\Omega \text{ cm}$, pH 5.7). OTS monolayer islands were first prepared on mica by LB deposition as previously described.¹⁵ Briefly, OTS was spread on water in a NIMA type 611 trough from a 0.3 mg mL^{-1} chloroform solution. When the monolayer was then transferred onto acid-treated mica at a surface pressure of 5 mN m^{-1} , islands of OTS were formed. The substrates were then immersed for 60 min in a 2.5 vol % solution of FTS in toluene in a dry nitrogen atmosphere. A continuous monolayer phase of FTS self-assembled between

the islands. The samples were rinsed with toluene and heated again in an oven at 100°C for 45 min.

The purified bacteriophage T4 and its tail tubes were prepared as described by Duda and Eiserling¹⁶ and diluted to about $0.1 \mu\text{g mL}^{-1}$ prior to use. Delipidated BSA obtained from Sigma Chemical Co. was used without further purification to prepare an aqueous solution at a concentration of $0.04 \mu\text{g mL}^{-1}$. Imaging studies were performed with a Park Scientific Instruments Autoprobe AFM. The experiments were initiated by depositing drops of the solutions on the substrates with a syringe. Two procedures were used to study the adsorption: (a) The samples were allowed to dry at ambient temperature in air and then were imaged in air; (b) the adsorption was directly observed by imaging under water. In this case the drop, which had a contact angle $>90^\circ$, was sandwiched between the substrate and the window of the cartridge from the Park open liquid cell. A commercial (Park Scientific Instruments) V-shaped silicon nitride cantilever tip with a spring constant of 0.05 N m^{-1} was used for all measurements. The vertical bending and lateral torsion of the cantilever were monitored by reflecting a laser beam from the end of the cantilever onto a four-segment photodetector so that the topographic and frictional force images of the samples could be obtained simultaneously and independently of each other. To minimize drift during the imaging, the microscope and the sample were allowed to thermally stabilize for 20 min. All measurements were carried out with a $5\text{-}\mu\text{m}$ scanner. The line scan speed was 2–4 Hz with 512 pixels. To reduce tip damage, the force was adjusted to the smallest possible value at which the samples could be imaged,

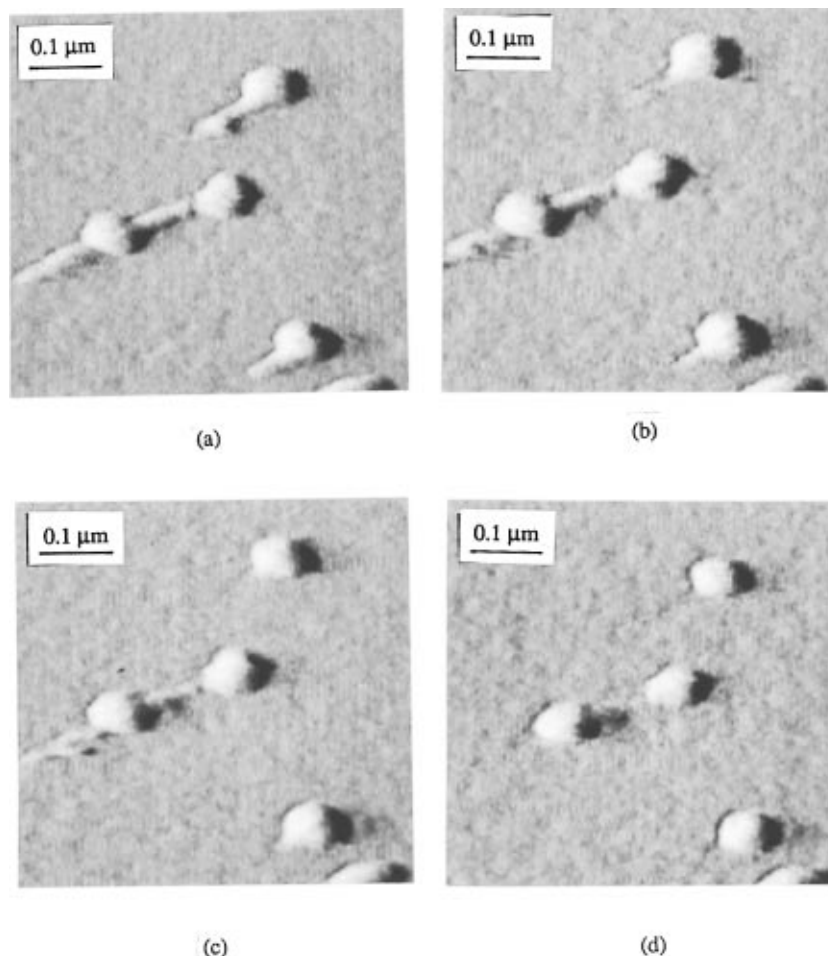


Figure 4. AFM images of tube-baseplates deposited from $0.1 \mu\text{g/mL}$ -solution onto the CF_3 -terminated surface. The images were taken after (a) 2, (b) 4, (c) 6, and (d) 10 scans. The loading force was 5 nN.

typically <4 nN. With the exception of flattening, the images shown here have not been enhanced.

Results and Discussion

The organization of the substrate can be seen in Figure 1, which is a typical topographic AFM image in air of purified T4 tail tubes adsorbed on the organosilane monolayer. The CH₃-terminated islands are smooth (rms roughness of 0.2–0.3 nm); the surrounding CF₃-terminated phase consists of grains ~0.02 μ m in diameter. High-resolution imaging reveals no evidence of crystallinity in either the OTS or FTS, in agreement with X-ray diffraction studies of LB-deposited OTS monolayers¹⁷ and self-assembled FTS monolayers.¹⁸

As can be seen from Figure 1, the tail tubes are preferentially adsorbed on the CF₃-terminated surface. The preference of the tubes for the perfluorinated surface is not an artifact of the drying. When mixed solutions of BSA and T4 tubes are deposited on the patterned monolayers, the tubes adhere to the CF₃-terminated surface and the BSA is adsorbed on the CH₃-terminated islands, Figure 2. This preference of BSA for CH₃-terminated surfaces is in accord with previous studies.¹⁰

It is known that the T4 tubes are 9.8 nm wide and 98 nm long.¹⁹ The average width of the tubes measured in the AFM images is 43 ± 2 nm. Much of the difference in the widths can be attributed to the geometrical effect of the AFM tip. If one assumes that the tip is a sphere of diameter D and that the tube is a cylinder of diameter d , the apparent width W can be calculated from the relation²⁰ $W = 2(Dd)^{1/2}$. The value of D given by the manufacturer is 40 nm, so the apparent width corresponds to $d = 12$ nm, reasonably close to the literature value. The measured height of the tube is unaffected by the tip size, and we find that it ranges from 9.4 to 10.3 nm, suggesting that the tubes are not compressed at the tip force employed for scanning or grossly distorted by the adsorption and drying.

Although broadening by the tip affects the image resolution, there is evidence of the finial bulge, an increase of the radius by about 4 nm on one end of the tubes, which has been seen by electron microscopy.²¹ Tube dimers, which are formed by linking two fibers that project from one end of the tubes, are also clearly visible in Figure 1. The angle between the tubes in a dimer varies from 80° to 180°, in agreement with electron microscopy measurements. However, the 2–3 nm wide fibers on one end of the tubes are not resolved by AFM.

Figure 3 shows a typical AFM image of the tail tubes with baseplates. The characteristic T-shaped tube-baseplates are clearly observed on the CF₃-terminated surface. The baseplates are more flexible than the rigid tubes. For example, negatively stained baseplates exhibit a dish shape and can undergo a transition from a hexagonal to a star-shaped configuration under the influence of the host bacterial cell,²² while freeze-etched baseplates appear in a knob configuration.²³ Here, Figure 4, we find that most of the baseplates exhibit a knob configuration but dish-shaped baseplates can occasionally be observed. Tail tubes joined to baseplates are stable when the loading force applied on the tip is <4 nN, but if the force is >5 nN, the tubes are gradually removed from the baseplates during repeated scans, even though the baseplates are not displaced. In this situation the tip acts like a knife to cut the tube from the baseplate.

Images of complete T4 in air are shown in Figure 5. The CH₃-terminated surface also resists T4 adsorption. Adsorbed T4 can be repeatedly imaged if the loading force is <4 nN. The head, tail, and probably three fibers of the phage are observed in the AFM image (Figure 5a). The head height

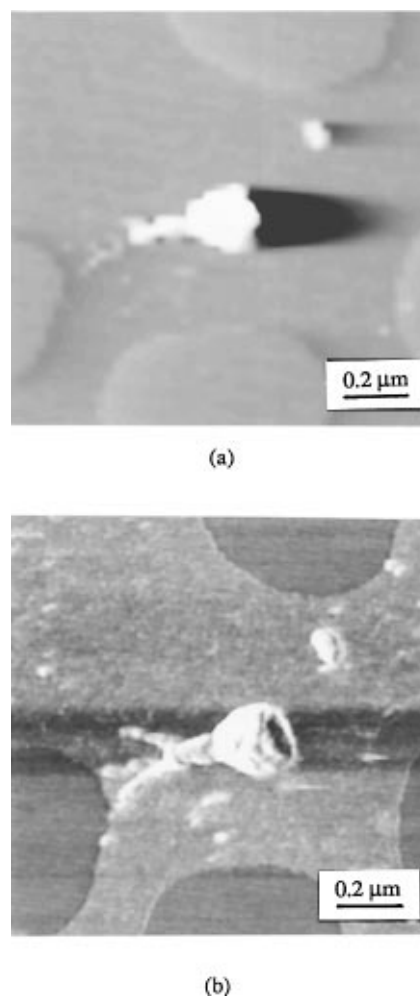


Figure 5. AFM (a) and FFM (b) images of individual T4. The two images were obtained simultaneously during scanning.

measured from the cross-sectional profile is about 71 nm, which is close to the known value, 75 nm. Figure 5b is a frictional force microscopy (FFM) image of T4 that was taken simultaneously with the AFM image. The resolution in the FFM images of T4 is better than that in topographic mode. Although the apparent dimensions of the head (120 nm length and 100 nm width) are affected by tip broadening, the ratio of the head length to width is close to the expected value. In addition, partial collapse of the head structure due to air-drying is also visible. The tail structures (neck and baseplate), which are not detected by the AFM, are better resolved by the FFM. The better resolution may be attributable to the high sensitivity of the frictional force to the chemical nature of the T4 surface. Recent studies have demonstrated the sensitivity of FFM to different chemical groups.^{24,25} Images of T4 made under water, Figure 6, also show that the phage is adsorbed on the CF₃ surface.

Figure 7a shows a FFM image of a giant T4 (a T4 phage with a normal tail but an elongated head²⁶). The giant head is 250 nm long and is flatter than a normal head. It is known that the sheath around the tail tubes consists of the 144 copies of gp18 protein arranged in 24 annuli of six subunits each. These sheath annuli are visible on the tail surface, Figure 7a. The measured spacing of the annuli is about 8.9 nm, which from transition electron microscopy (TEM) is expected to be 4.1 nm. The doubling of the periodicity may perhaps be explained by a pairing of the annuli as a result of drying. This phenomenon is known to occur in air-dried samples of tobacco mosaic virus²⁷ although it has not been seen before in T4. Attempts to resolve

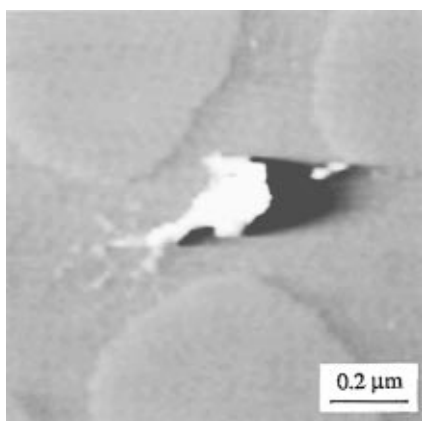
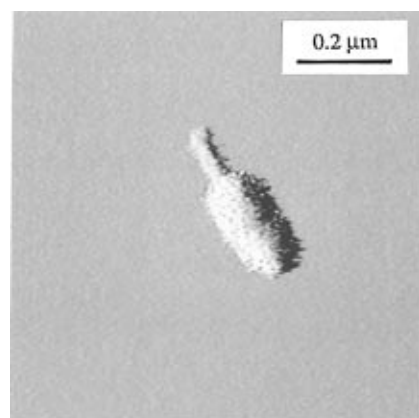
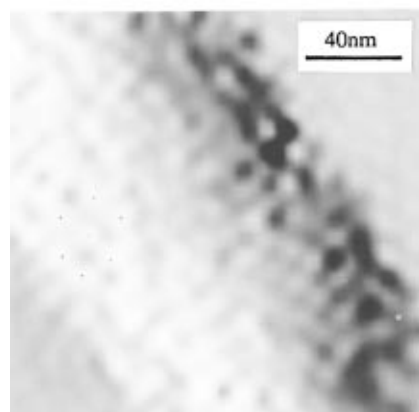


Figure 6. AFM image of T4 adsorbed on the patterned monolayer. The image was taken under water.



(a)



(b)

Figure 7. FFM images of a giant T4. (a) Image of a complete T4. (b) Image of the head surface.

the structure of the tail surface under water have not been successful. A higher resolution image of the head surface is shown in Figure 7b. The characteristic hexagonal capsid lattice of the head is evident. The lattice spacing from the FFM image, which is unaffected by the tip size, is about 15.8 nm. This value compares favorably with that obtained by TEM.

High-resolution scanning force microscopy images of individual biopolymers have been obtained in experiments in which

the polymer has been immobilized on a substrate by covalent bonding⁹ or by incorporating it into a membrane.⁸ Crystalline arrays of polymers, which are more easily imaged than individual molecules, have been imaged at 1 nm resolution.⁸ In our experiments, in which the samples have been prepared by simple adsorption onto a substrate from solution, features on isolated T4 as small as 4 nm have been observed and detailed organization on a scale smaller than 8 nm have been resolved by FFM, imaging markedly better than in previous AFM studies of T4.^{12–14} While the resolution is poorer than the 2–3 nm obtainable with standard electron microscopy, the procedure for preparing samples is much simpler, which offers significant advantages.

Acknowledgment. This work was supported by the National Science Foundation.

References and Notes

- (1) Engel, A. *Annu. Rev. Biophys. Biophys. Chem.* **1991**, *20*, 79.
- (2) Hansma, H. G.; Vesenka, J.; Siegerist, C.; Kelderman, G.; Morrer, H.; Sinsheimer, R. L.; Elins, V.; Bustamante, C.; Hansma, P. K. *Science* **1992**, *256*, 1180.
- (3) Weisenhorn, A. L.; Drake, B.; Prater, C. B.; Gould, S. A. C.; Hansma, P. K.; Ohnesorge, F.; Egger, M.; Heyn, S. P.; Gaub, H. E. *Biophys. J.* **1990**, *58*, 1251.
- (4) Prime, K. L.; Whitesides, G. M. *Science* **1991**, *252*, 1164.
- (5) Lösche, M.; Piepenstock, M.; Diederich, A.; Grünwald, T.; Kjaer, K.; Vaknin, D. *Biophys. J.* **1993**, *65*, 2160.
- (6) Karrasch, S.; Dolder, M.; Schabert, F.; Ramsden, J.; Engel, A. *Biophys. J.* **1993**, *65*, 2437.
- (7) Ohnishi, S.; Hara, M.; Furuno, T.; Sasabe, H. *Biophys. J.* **1992**, *63*, 1425.
- (8) Yang, J.; Tamm, L. K.; Tillack, T. W.; Shao, Z. F. *J. Mol. Biol.* **1993**, *229*, 286.
- (9) Wagner, P.; Kern, P.; Heyner, M.; Ungewickell, E.; Semenza, G. *FEBS Lett.* **1994**, *356*, 267.
- (10) Fang, J. Y.; Knobler, C. M. *Langmuir* **1996**, *12*, 1368.
- (11) Eiserling, F. A.; Black, L. W. In *Bacteriophage T4*; Karam, J. D., et al., Eds.; American Society for Microbiology: Washington, DC, 1994; p 209.
- (12) Kolbe, W. E.; Ogletree, D. F.; Salmeron, M. B. *Ultramicroscopy* **1992**, *42–44*, 1113.
- (13) Droz, E.; Taborrelli, M.; Wed, T. N. C.; Descouts, P. *Biophys. J.* **1993**, *65*, 1180.
- (14) Ikai, A.; Imai, K.; Yoshimura, K.; Tomitori, M.; Nishikawa, O.; Kokawa, R.; Kobayashi, M.; Yamamoto, M. *J. Vac. Sci. Technol.* **1992**, *B12*, 1478.
- (15) Fang, J. Y.; Knobler, C. M. *J. Phys. Chem.* **1995**, *99*, 10425.
- (16) Duda, R.; Eiserling, F. A. *J. Virology* **1982**, *43*, 714.
- (17) Bourdieu, L.; Daillant, J.; Chatenay, D.; Braslau, A.; Colson, D. *Phys. Rev. Lett.* **1994**, *72*, 1502.
- (18) Geer, R. E.; Stenger, D. A.; Chen, M. S.; Calvert, J. M.; Shashidhar, R.; Jeong, Y. H.; Pershan, P. S. *Langmuir* **1994**, *10*, 1174.
- (19) Duda, R. L.; Wall, J. S.; Hainfeld, J. F.; Sweet, R. M.; Eiserling, F. A. *Proc. Natl. Acad. Sci. U.S.A.* **1985**, *82*, 5550.
- (20) Zenhausern, F.; Adrian, M.; Ten Heggeler-Bordier, B.; Eng, L. M.; Descouts, P. *Scanning* **1992**, *14*, 212.
- (21) Duda, R.; Gingery, M.; Eiserling, F. A. *Virology* **1986**, *151*, 296.
- (22) Coombs, D. H.; Arisaka, F. In *Bacteriophage T4*; Karam, J. D., et al., Eds.; American Society for Microbiology: Washington, DC, 1994; p 259.
- (23) Benbasat, J. A.; Ruben, G. C.; Marx, K. J. *Biomol. Struct. Dynam.* **1990**, *7*, 773.
- (24) Overney, R. M.; Meyer, E.; Frommer, J.; Brodbeck, D.; Lüthi, R.; Howald, L.; Güntherodt, H. J.; Fujihira, M.; Takano, H.; Gotoh, Y. *Nature* **1992**, *357*, 133.
- (25) Wilbur, J. L.; Biebuyck, H. A.; MacDonald, J. C.; Whitesides, G. M. *Langmuir* **1995**, *11*, 825.
- (26) Doermann, A. H.; Pao, A. J. *Virol.* **1987**, *61*, 2835.
- (27) Durham, C. H.; Finch, J. T.; Klug, A. *Nature New Biology* **1971**, *229*, 37.